

Nonlinear Aspects of Hypersonic Boundary-Layer Stability on a Porous Surface

Ndaona Chokani*

Duke University, Durham, North Carolina 27708

and

Dimitry A. Bountin,[†] Alexander N. Shpilyuk,[‡] and Anatoly A. Maslov[§]

Russian Academy of Sciences, 630090, Novosibirsk, Russia

The nonlinear aspects of the stabilization of the second-mode disturbance using a passive, ultrasonically absorptive coating (UAC) of regular microstructure are studied using bispectral analysis. The experimental data consist of hot-wire measurements made in artificially excited wave packets that are introduced into the hypersonic boundary layer on both solid and porous surfaces. The bispectral measurements show that the subharmonic and harmonic resonances of the second mode are significantly modified. The harmonic resonance, which is quite pronounced in the latter stages of the hypersonic boundary layer on solid surfaces, is completely absent on the porous surface. The degree of nonlinear phase locking that is associated with the subharmonic resonance and identified on the solid surface is substantially weakened on the porous surface. This nonlinear interaction persists farther downstream on the porous surface than on the solid surface; however, unlike on the solid surface, there are no strongly preferred interaction modes. The spectral measurements, made in previous work, show that the first mode is moderately destabilized on the porous surface. The bispectral measurements presented here identify a nonlinear interaction that is associated with the destabilized first mode; however, this is observed to be a very weak nonlinear interaction that has no deleterious effect on the performance of the UAC.

Nomenclature

$B(f_1, f_2)$	=	bispectrum
$b^2(f_1, f_2)$	=	bicoherence spectrum
f	=	frequency, kHz
f_1	=	frequency at center of first-mode packet
f_{II}	=	frequency of most amplified second mode
f_N	=	Nyquist frequency
f_1, f_2, f_3	=	frequencies of wave triad
$P(f)$	=	power spectrum
Re_x	=	Reynolds number based on axial distance x
T	=	time period
t	=	time
U_e	=	boundary-layer edge velocity
$X(f)$	=	complex Fourier transform
x	=	axial distance measured from tip of cone model
δ	=	boundary-layer thickness
θ	=	phase of wave of frequency f
$\langle \rangle$	=	ensemble-averaged quantity

Superscript

*	=	complex conjugate
---	---	-------------------

Presented as Paper 2004-0255 at the AIAA 42nd Aerospace Sciences Meeting, Reno, NV, 5–8 January 2004; received 25 March 2004; revision received 11 August 2004; accepted for publication 11 August 2004. Copyright © 2004 by Ndaona Chokani and Anatoly Maslov. Published by the American Institute of Aeronautics and Astronautics, Inc., with permission. Copies of this paper may be made for personal or internal use, on condition that the copier pay the \$10.00 per-copy fee to the Copyright Clearance Center, Inc., 222 Rosewood Drive, Danvers, MA 01923; include the code 0001-1452/05 \$10.00 in correspondence with the CCC.

*Research Professor, Mechanical Engineering and Materials Science Department, 144 Hudson Hall; ndaona.chokani@duke.edu. Associate Fellow AIAA.

[†]Research Assistant, Institute of Theoretical and Applied Mechanics, Siberian Branch.

[‡]Senior Researcher, Institute of Theoretical and Applied Mechanics, Siberian Branch.

[§]Deputy Director and Professor, Institute of Theoretical and Applied Mechanics, Siberian Branch. Member AIAA.

I. Introduction

IN axisymmetric and two-dimensional boundary layers at hypersonic speeds, the transition from laminar-to-turbulent flow occurs as a result of the presence of second-mode disturbances. The boundary-layer transition occurs, for example, in axisymmetric boundary layers on ballistic reentry vehicles and in two-dimensional boundary layers on the forebody of airbreathing hypersonic vehicles. The location of transition is of critical importance in the design of such hypersonic vehicles as both the aerodynamic heating and skin friction are higher in transitional and turbulent flows compared to laminar flow. Whitehead¹ noted, for example, that if the National Aerospace Plane's boundary layer were fully laminar, compared to fully turbulent, then the ratio of payload-to-gross weight could have been increased by 100%. It is quite evident that a delay of the transition from a laminar-to-turbulent state will facilitate the optimal design of hypersonic vehicles.

The generally accepted view is that in a low-disturbance environment and in the absence of wall roughness transition is caused by the amplification of wave-like disturbances that are present in the boundary layer.² In the case of axisymmetric/two-dimensional hypersonic boundary layers, the most dominant disturbance is the second mode. The second-mode disturbance is the result of an inviscid instability that arises as a result of the presence of a region of boundary-layer flow that is supersonic relative to the disturbance's phase velocity. The second mode is acoustic in character, as the relative supersonic boundary-layer region acts like an acoustic waveguide for the acoustic rays that are reflected between the relative sonic line and the wall. The dominant role of the second mode in causing hypersonic transition is very well established. Malik³ has recently used the parabolized stability equations with finite-rate chemistry to analyze the experimental data for high-altitude, hypersonic, flight cases; it is observed that the transition is caused by second-mode disturbances. Therefore hypersonic boundary-layer transition control concepts that address the second-mode disturbance are of immense technological importance.⁴

Fedorov and Malmuth⁵ used linear stability theory (LST) to propose that the transition in hypersonic flow can be delayed by suppressing the second-mode disturbances through the use of a suitably designed porous coating. This passive, ultrasonically absorptive coating (UAC) consists of a thin porous layer that is flush mounted

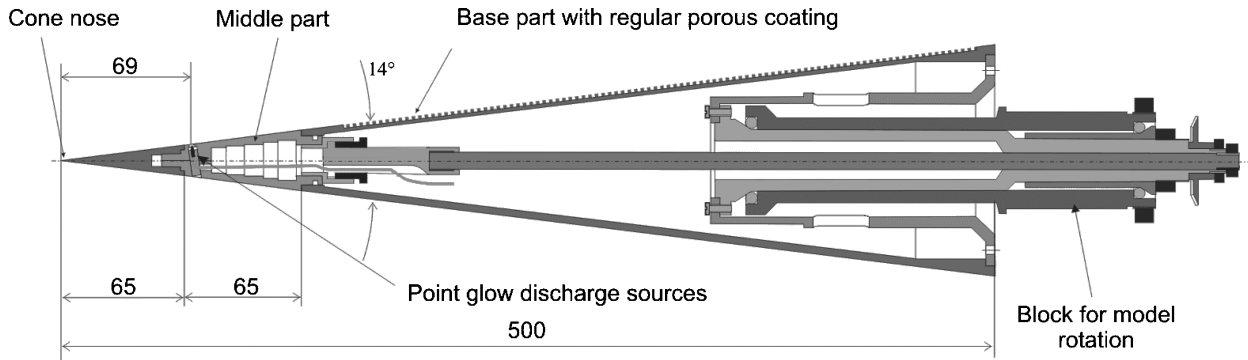


Fig. 1 Schematic of model with electric glow discharge source.

onto the solid surface. Rasheed et al.⁶ provided the first experimental verification of this passive transition control concept. The results of experiments conducted in the GALCIT T5 Hypervelocity Free-Piston Shock Tunnel, using a 5-deg half-angle sharp cone with a thin porous coating of random microstructure, showed that the transition Reynolds numbers are dramatically increased. Although only the onset of transition was measured, the experiments qualitatively confirmed the LST predictions of Fedorov and Malmuth.⁵ The first direct experimental evidence that the porous coating stabilizes the second mode was obtained in experiments conducted in the T-326 hypersonic wind tunnel at the Institute of Theoretical and Applied Mechanics (ITAM) of the Siberian Division of the Russian Academy of Sciences.⁷ These experiments were performed on a 7-deg half-angle sharp cone that was partially covered with a UAC of random microstructure. In a second series of experiments at ITAM, the stabilization of the second-mode disturbance using an UAC of regular microstructure was also examined.⁸ The experimental measurements of amplitudes of the second-mode disturbances show relatively good agreement with the theoretical predictions and confirm that the porous coating indeed stabilizes the second mode. However a comparison of experiment and theory shows that the theory underestimates the stabilization effect of the UAC. A plausible source of the discrepancy is the nonlinear mechanisms that occur in the hypersonic boundary layer on the porous surface. There is for example the interesting observation in the experiment that in conjunction with the stabilization of the second mode the UAC is moderately destabilizing to the first mode.

There are various possible physical nonlinear mechanisms for the redistribution of energy between disturbance modes. The most efficient energy transfer between modes occurs when there is nonlinear phase locking; nonlinear phase-locked interactions can be measured and documented using the bispectral analysis. Kimmel and Kendall⁹ and Chokani¹⁰ used bispectral analysis to identify the generation of the harmonic in naturally occurring second-mode disturbances in an initially laminar hypersonic boundary layers. The subharmonic resonance of naturally occurring and artificially generated second-mode disturbances was recently identified by Shpiyuk et al.^{11,12}

The objective of the present paper is to clarify the mechanisms of hypersonic transition control using a porous coating. This is accomplished by applying the bispectral analysis technique to the hot-wire measurements of artificially excited wave packets that are introduced into the hypersonic boundary layer on both solid and porous surfaces. The experimental setup is briefly described in the following section; the interested reader is referred to Fedorov et al.⁸ for more complete details. The bispectral analysis technique is then described in a subsequent section; we describe in this section only the elements that are essential to interpret our results; the details of the technique is discussed in Kim and Powers¹³ and further details of the application of the technique are presented in Kimmel and Kendall⁹ and Chokani.¹⁰ The measurements of the nonlinear phase locking are then presented in the results and discussion section. Our analysis shows the intriguing result that the energy saturation of the second mode on the UAC is a result of an enhanced subharmonic resonance process. This nonlinear interaction persists far downstream

on the porous surface, albeit at a reduced level; this is in contrast to the solid surface where the subharmonic resonance is more intense for a smaller streamwise extent.

II. Experimental Method

The experiments are performed in the hypersonic wind tunnel T-326 at ITAM. The freestream Mach number is 5.95 (± 0.02), the stagnation pressure 1.0 MPa ($\pm 0.06\%$), and the total temperature 390 K ($\pm 0.25\%$), which yield a unit Reynolds number of $(11.5\text{--}12.3) \times 10^6/\text{m}$. The model, which has an overall length of 500 mm, is a 7-deg half-angle sharp-nosed cone that consists of four parts (Fig. 1). The first 65 mm length constitutes the sharp nose. An electric glow discharge actuator is contained within the 65-mm-long, middle part. The back part, 370 mm in length, contains the solid and porous surfaces. Finally there is an aft part, which contains a motorized block to rotate the model about its axis. One longitudinal half of the back part is a solid surface. (Surface roughness is approximately $5 \mu\text{m}$.) The other longitudinal half is a 450- μm -thick, perforated sheet, which constitutes the porous surface; the leading edge of the porous surface is 182 mm from the cone tip. The diameter of the holes on the side of the porous surface that is exposed to the flow is $50 \mu\text{m}$ ($\pm 6 \mu\text{m}$), and the holes' diameter is $64 \mu\text{m}$ ($\pm 6 \mu\text{m}$) on the side that is flush mounted to the cone's surface. The spacing between the holes is $100 \mu\text{m}$ ($\pm 4 \mu\text{m}$), which yields, based on the mean hole diameter, an open area (porosity) of 0.2. The model is installed at zero angle of attack; the estimated misalignment between the cone axis and the freestream direction is less than 0.1 deg.

Artificial disturbances are generated by a high-frequency glow discharge. The disturbance frequency is 275 kHz, which corresponds to the second-mode disturbance under natural conditions on the solid surface. The artificial disturbances emanate from an orifice, 0.4 mm in diameter, which is located 69 mm downstream of the model's tip. The dominant component of these artificially excited wave packets is two-dimensional.⁸

A custom-built constant-current anemometer is used to operate a hot-wire and measure mass flow fluctuations. The hot-wire probes are made of tungsten wire of 5- μm diam and 1-mm length. The overheat ratio is 0.5; and the frequency response of hot-wire anemometer is 500 kHz. The output of the anemometer is measured using a 12-bit ADC with a sampling frequency of 5 MHz. The hot-wire measurements are made along a streamwise ray at the maximum rms disturbance location in the center of the wave packets. At each measurement station, 98 time series of 4096 samples are acquired.

III. Bispectral Analysis

When two unstable modes at frequencies f_1 and f_2 interact to form a third mode of frequency f_3 , such that $f_3 = f_1 \pm f_2$, then the phase of the third mode is equal to the sum (or difference) of the two interacting modes $\theta_3 = \theta_1 \pm \theta_2$. This phase relationship implies that the three modes become phase coherent over many statistical realizations. The nonlinear phase locking between the three modes can then be detected by measuring their phase coherence.

The bicoherence spectrum, also called the bicoherence, provides a measure of the phase coherence and thus of the nonlinear phase locking. The bicoherence is defined here as

$$b^2(f_1, f_2) = \frac{|B(f_1, f_2)|^2}{P(f_1)P(f_2)P(f_3)} \quad (1)$$

where the bispectrum is given as

$$B(f_1, f_2) = \langle X(f_1)X(f_2)X^*(f_3) \rangle \quad (2)$$

and the power spectrum as

$$P(f) = \langle X(f)X^*(f) \rangle \quad (3)$$

The bicoherence $b^2(f_1, f_2)$ is a two-dimensional function of frequency. The magnitude of the bicoherence is therefore plotted as constant-level contours in the f_1, f_2 plane. The frequencies of the triad modes involved in the identified nonlinear phased-locked interactions are then given by f_1, f_2 , and $f_1 \pm f_2$. The bicoherence is symmetric in the f_1, f_2 plane about the three lines $f_1 = f_2, f_2 = 0$, and $f_1 + f_2 = f_N$. The bicoherence is bounded by values of zero and one. When there is no phase locking, the value of the bicoherence is zero. When the degree of phase locking is high, the bicoherence is then close to one; however, the value of the bicoherence is also dependent on the signal-to-noise ratio of the measured data.

The spectral moments, Eqs. (2) and (3), are averaged to reduce the variance in the moments, and a Hanning window is used to reduce the spectral leakage. In the present work, the averaged bispectrum estimate is obtained from nonoverlapping fast Fourier transform blocks of length 512; therefore, the frequency resolution in the bicoherence spectrum is 9.8 kHz.

IV. Results and Discussion

A sequence of Fourier spectra measured at eight different streamwise stations, on solid and porous surfaces, is presented in Figs. 2 and 3 to illustrate the most salient features of the UAC stabilization. We note here that the Fourier spectra do not retain any phase information, but for the sake of completeness a brief discussion of these spectra is nevertheless warranted. A more detailed discussion of the Fourier spectra is presented in Fedorov et al.^{7,8}

On the solid surface (Fig. 2), the Fourier spectra show that the second mode is the dominant disturbance. The frequency of the second mode is known to be tuned to the boundary-layer thickness U_e/δ (Refs. 14 and 15). Therefore the frequency of the second mode

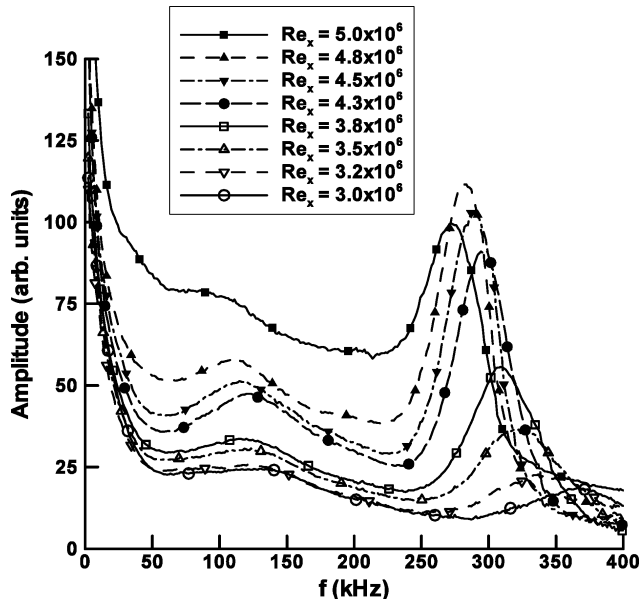


Fig. 2 Streamwise evolution of disturbance spectra on solid surface.

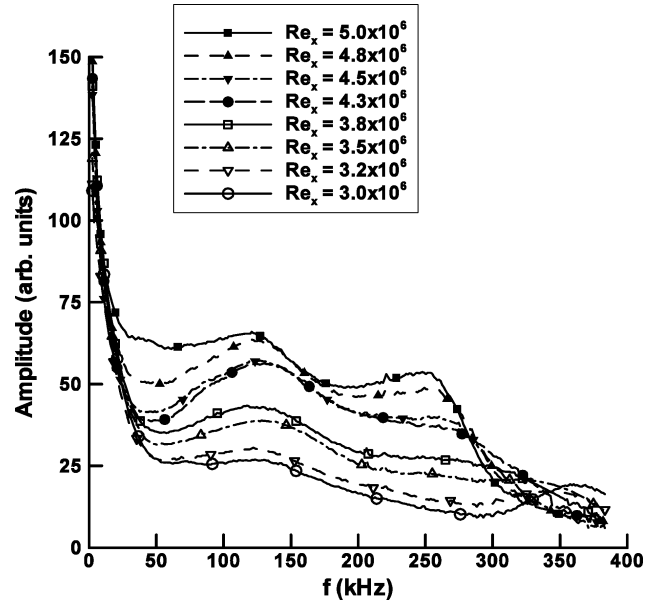


Fig. 3 Streamwise evolution of disturbance spectra on porous surface.

decreases in the streamwise direction; f_{II} is ≈ 325 kHz, at the most upstream station and 270 kHz at the most downstream station. The amplitude of the second mode also increases downstream and at a given station is always larger than the amplitude of the first mode; the first mode is within the frequency band $f_I \approx 75\text{--}125$ kHz. At the most downstream measurement station $Re_x = 5 \times 10^6$, the Fourier spectra show a filling in of the valleys between the unstable modes, which is indicative of the first stages of the breakdown to turbulent flow.

On the porous surface (Fig. 3), the second mode is effectively stabilized. At all measurement stations, the amplitude of the second mode is very much smaller on the porous surface compared to the solid surface. The stabilized second mode shows only a modest change in its amplitude in the downstream direction: this modest change is reminiscent of the saturation in the energy of the second mode when nonlinear interactions are significant.¹⁰ In contrast to the solid surface, on the porous surface at a given measurement location the amplitude of the first mode is larger than that of the second mode. At the most upstream station the destabilizing effect of the UAC on the first mode is clearly evident as the amplitude of the first mode is smaller on the solid surface, <25 , compared to its amplitude on the porous surface, >25 . On the solid surface, the differences in the structure of the energy in the sidebands around the second mode and the redistribution of the energy into subharmonic frequencies have been shown to be evidence of significant nonlinear phase locking.^{11,12}

The bispectral measurements that are used to measure and document the nonlinear phase locking are presented next. The symmetry of the bicoherence has already been noted; however, for convenience in the present work the bicoherence in the positive quadrant of the f_1, f_2 plane with frequencies less than 400 kHz is plotted. The bispectral measurements are presented (Figs. 4–9), for six streamwise locations, $x = 211, 245, 269, 286, 304, \text{ and } 315$ mm. In each figure both the measurements on solid and porous surfaces are presented. In the plots the dashed line shows the line of symmetry $f_1 = f_2$. The diagonal solid line that shows the relation $f_1 + f_2 = f_{II}$ is also shown; this relation is significant because it is indicative of the subharmonic resonance of the second mode on the solid surface. Note that the frequency of the most amplified second mode changes with streamwise location. The contour interval in the plot of the bicoherence is 0.025; at a given measurement station the same range of contours levels is shown for both the solid and porous surfaces so that the relative degree of nonlinear phase locking caused by the UAC is indicated and the nonlinear aspects of the stabilization can also be assessed.

The bicoherence spectra at $x = 211$ mm are shown in Fig. 4. In both plots the levels of the bicoherence are insignificant, less

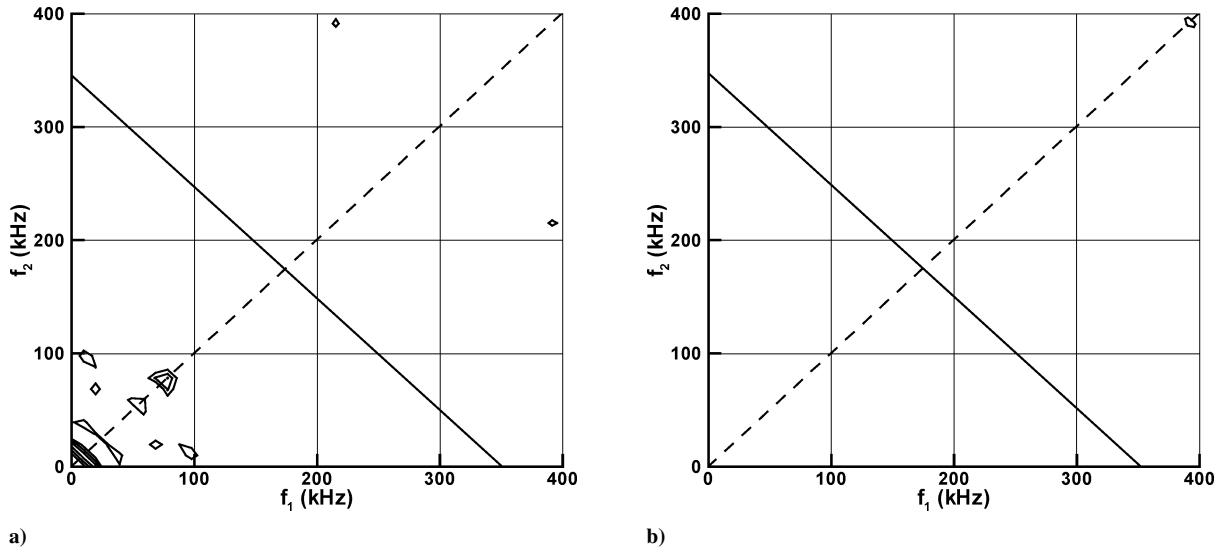


Fig. 4 Bicoherence spectra at $x = 211$ mm: a) solid and b) porous surface.

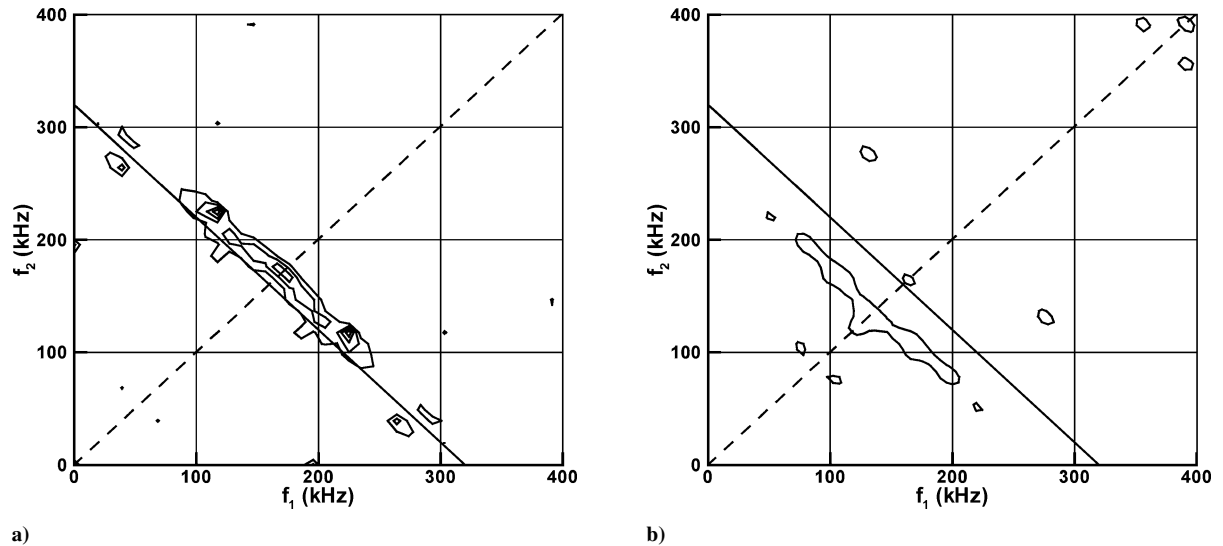


Fig. 5 Bicoherence spectra at $x = 245$ mm: a) solid and b) porous surface.

than 0.05; therefore, at this location no nonlinear phase locking is detected, and the spectral evolution is linear.

At $x = 245$ mm (Fig. 5), a significant degree of nonlinear phase locking is measured on the solid surface, but it is weak on the porous surface. The frequency of the most unstable second mode on the solid surface is $f_{II} = 320$ kHz; although the observed nonlinear phase locking, $f_1 + f_2 \approx 335$ kHz on the solid surface (Fig. 5a), involves a somewhat higher frequency than f_{II} , this higher frequency is within the spectral resolution of the bispectrum estimate. The most significant nonlinear interaction occurs at $(f_1, f_2) = (230 \text{ kHz}, 110 \text{ kHz}) \approx (f_{II} - f_1, f_1)$. As just discussed, the bicoherence is symmetric in the f_1, f_2 plane; therefore, difference-mode interactions of the form $f_3 - f_1 = f_2$ and $f_3 - f_2 = f_1$ are also mapped onto the sum-mode interaction, $f_3 = f_1 + f_2$. However, because the frequencies of the unstable first mode f_I and second mode f_{II} are known, there is no ambiguity in distinguishing between sum-mode and difference-mode interactions. Therefore on the solid surface a weak nonlinear phase locking between the first and second mode is identified. The initial stages of the subharmonic resonance of the second mode are evident from the slight peak at $(f_1, f_2) = (165 \text{ kHz}, 165 \text{ kHz}) \approx (f_{II}/2, f_{II}/2)$. Although no significant nonlinear phase locking is detected on the porous surface (Fig. 5b), the initial stage of nonlinearity is observed to occur; this involves frequencies that are significantly lower than the frequency of the most unstable second mode on the solid surface.

The nonlinear phase locking on the porous surface is more pronounced at the next measurement station, $x = 269$ mm (Fig. 6b). The frequency of the most unstable second mode on the solid surface is $f_{II} = 300$ kHz. The nonlinear phase locking $f_1 + f_2 \approx 280$ kHz on the porous surface shows no preferred mode interactions, but involves a broad range of frequencies, 90–190 kHz. The degree of nonlinear phase locking on the porous surface is smaller than that observed on the solid surface (Fig. 6a). Additionally the strong subharmonic resonance $(f_1, f_2) = (150 \text{ kHz}, 150 \text{ kHz}) \approx (f_{II}/2, f_{II}/2)$ and the phase-locked interaction between the first and second modes $(f_1, f_2) = (200 \text{ kHz}, 100 \text{ kHz}) \approx (f_{II} - f_1, f_1)$ that are present on the solid surface are absent on the porous surface. This is a direct measure of the effectiveness of the UAC in suppressing nonlinear interactions. Further evidence of the effectiveness of the UAC is the observation that the harmonic phase locking $(f_1, f_2) = (290 \text{ kHz}, 290 \text{ kHz}) \approx (f_{II}, f_{II})$ that is present on the solid surface is completely absent on the porous surface. This harmonic interaction was first quantified in the bispectral measurements of Kimmel and Kendall⁹; in a subsequent study, Chokani¹⁰ observed that this harmonic interaction is very pronounced when wall cooling has destabilized the second mode. The fact that the UAC suppresses this very dangerous nonlinear effect confirms the tremendous potential of UAC for practical applications of hypersonic transition control.

At the more downstream station $x = 286$ mm (Fig. 7), we have further confirmation of the stabilization of the second mode using the

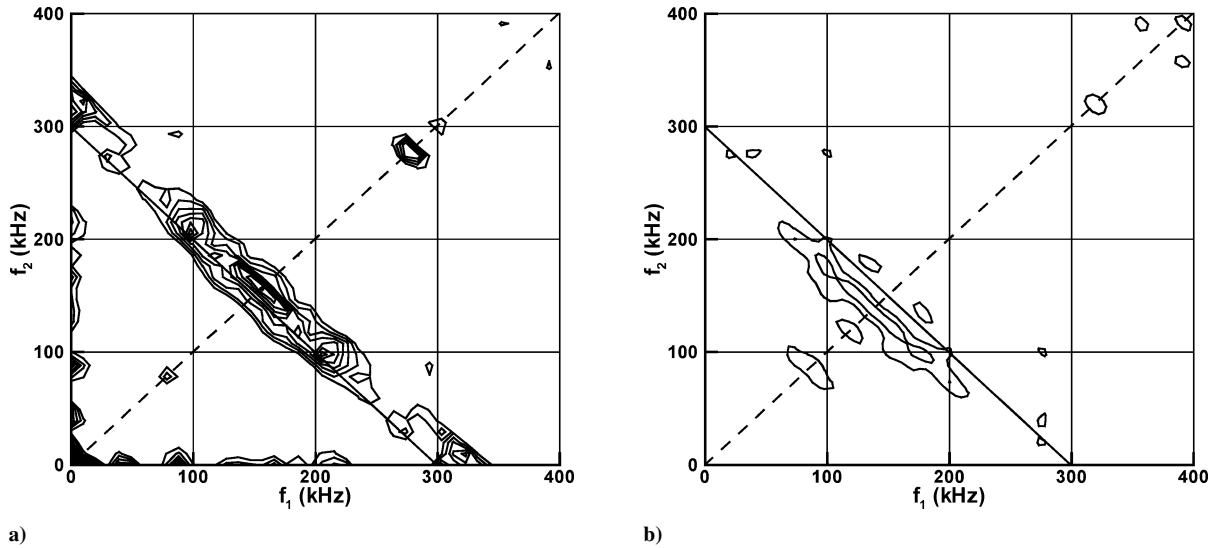


Fig. 6 Bicoherence spectra at $x = 269$ mm: a) solid and b) porous surface.

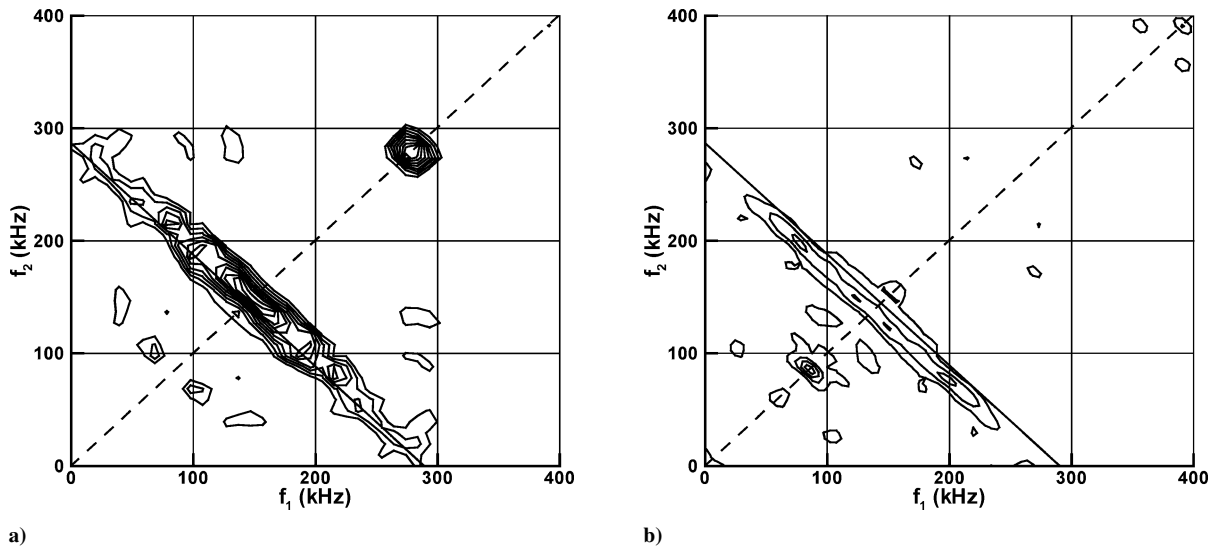


Fig. 7 Bicoherence spectra at $x = 286$ mm: a) solid and b) porous surface.

UAC. Note again that the range and intervals of the contour levels in both parts of the figure are the same. It is thus quite clear that degree of nonlinear phase locking is substantially reduced on the porous surface compared to the solid surface. The harmonic generation associated with the second mode $f_{II} = 290$ kHz is completely suppressed on the porous surface. On the solid surface (Fig. 7b) the nonlinear phase locking is also quite large between the second mode and its subharmonic $(f_1, f_2) = (140 \text{ kHz}, 140 \text{ kHz}) \approx (f_{II}/2, f_{II}/2)$ and between the first and second modes $(f_1, f_2) = (210 \text{ kHz}, 90 \text{ kHz}) \approx (f_{II} - f_I, f_I)$. There are also increased levels of nonlinear phase locking between triads in the complete range of frequencies up to f_{II} ; this indicates that the valleys between the spectral peaks are filling in, and the boundary layer is therefore entering into the initial stages of the breakdown to turbulence. This situation can be contrasted with the state of the boundary layer on the porous surface, which is observed to remain quite laminar (see also the shadow-graph images presented in Fig. 7 of Ref. 6). The bispectral measurements on the porous surface (Fig. 7b) show that the nonlinear phase locking involves a limited range of frequencies, 50–230 kHz. The energy transfer between the wave triads in this frequency range is therefore enhanced, which explains the filling of the spectrum that is observed in Fig. 3. However, on the porous surface, unlike the solid surface, there are no preferred mode interactions; it is therefore evident that the UAC is effective in substantially weakening the

nonlinear interactions involving the second mode, its subharmonic, and the first mode.

Fedorov et al.^{7,8} observed that the first mode is marginally destabilized by the UAC. This is evident in the bispectral measurements (Fig. 7b) on the porous surface where nonlinear phase locking, albeit of a weak intensity, involving only the first mode $(f_1, f_2) = (90 \text{ kHz}, 90 \text{ kHz}) \approx (f_I/2, f_I/2)$ is observed. This interaction is of a “classical” type in the sense that it resembles the subharmonic resonance of Tollmein–Schlichting-like (TS-like) waves observed in subsonic laminar boundary layers by Kachanov and Levchenko,¹⁶ and Saric et al.,¹⁷ and in supersonic boundary layers by Kosinov et al.¹⁸ In the subsonic and supersonic flows on solid surfaces, the unstable disturbances are TS-like waves; similarly in the hypersonic flow over the porous surface the amplitude of the vortical-type, first mode is larger than the amplitude of the acoustic-type, second mode. Thus although the first mode is destabilized and there is no discernible change in the amplitude of the second mode, the bispectral measurements indicate that the nonlinear effects involving the destabilized first mode are quite weak. This is evident as the first-mode interaction $(f_1/2, f_1/2)$ is absent at the next measurement station $x = 304$ mm, (Fig. 8b) and weak at the most downstream station $x = 315$ mm (Fig. 9b). Throughout this measurement range the plots of the bicoherence spectra are characterized by a relatively high degree of nonlinear phase locking associated with the second mode. This would suggest

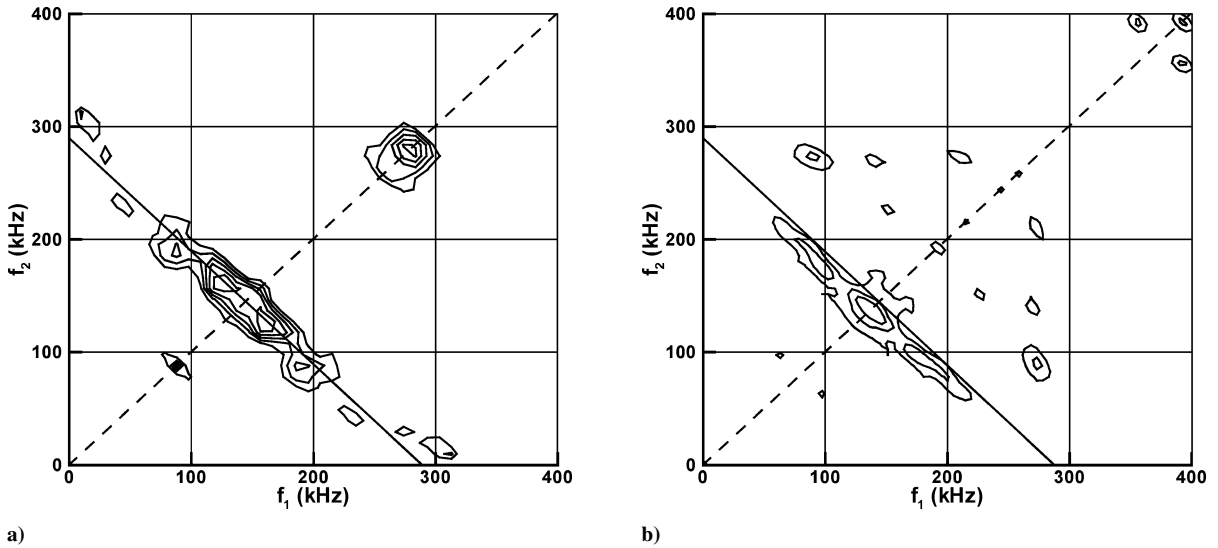


Fig. 8 Bicoherence spectra at $x = 304$ mm: a) solid and b) porous surface.

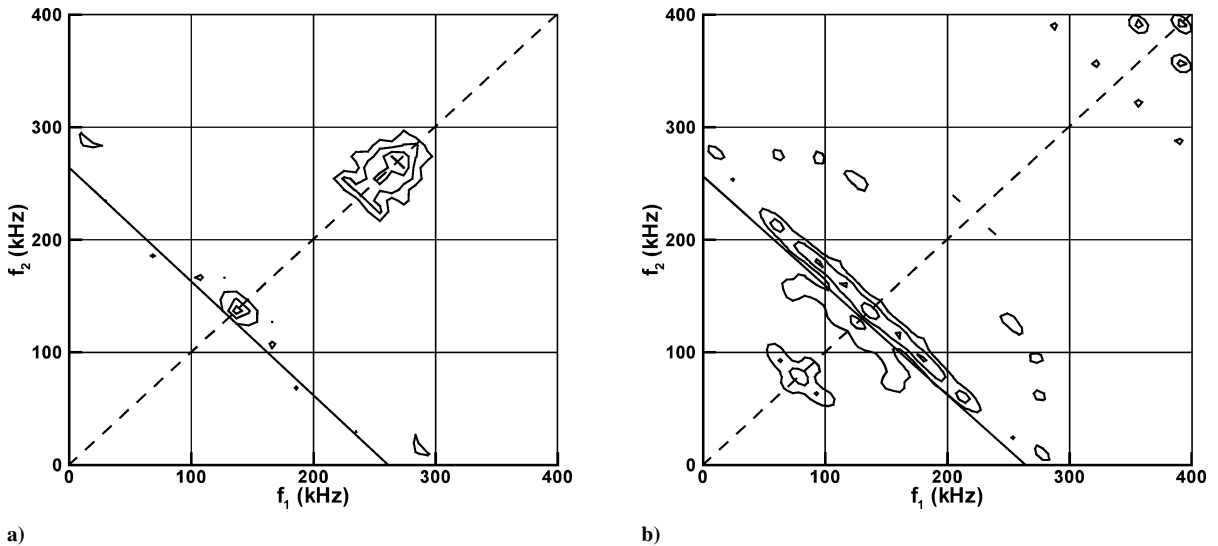


Fig. 9 Bicoherence spectra at $x = 315$ mm: a) solid and b) porous surface.

that a tailoring of the UAC could be used to further enhance its effectiveness for hypersonic transition control.

On the solid surface, at $x = 304$ mm (Fig. 8a) the degree of nonlinear phase locking that is associated with the subharmonic ($f_1/2$, $f_1/2$) and harmonic (f_{II} , f_{II}) resonances are comparable. However on the porous surface (Fig. 8b) only a weak subharmonic resonance ($f_1/2$, $f_1/2$) is observed, together with a weak difference-mode interaction (f_1 , f_2) = (180 kHz, 90 kHz) \approx ($f_{II} - f_1$, f_1), which involves both the first and second modes; these nonlinear effects closely resemble the nonlinear interactions that are observed more upstream on the solid surface at $x = 245$ mm (Fig. 5). This further illustrates the effectiveness of UAC in delaying the nonlinear phenomena that lead to hypersonic boundary-layer transition.

At the last measurement station $x = 315$ mm, the subharmonic and harmonic resonant interactions persist on the solid surface (Fig. 9a). The harmonic interaction is suppressed on the porous surface (Fig. 9b). It is also observed that there is no preferred nonlinear interaction along $f_1 + f_2 \approx f_{II} \approx 260$ kHz, and the subharmonic interaction of the first mode (f_1 , f_2) = (85 kHz, 85 kHz) \approx ($f_1/2$, $f_1/2$) is observed to be very weak.

V. Conclusions

The bispectral analysis of the hot-wire data made in a hypersonic boundary layer on an ultrasonically absorptive coating of regular microstructure is presented. The experiments are made on a 7-deg

half-angle sharp cone at zero angle of attack in a Mach 6 wind tunnel. Artificially excited wave packets that are generated at the frequency of the second mode are used to introduce disturbances into the hypersonic boundary layer. The bispectral measurements reveal several nonlinear aspects of the stabilization of the second mode disturbance using the ultrasonically absorptive coating:

1) The subharmonic and harmonic resonances of the second mode that are observed on solid surfaces are significantly modified on the porous surface.

2) The harmonic resonance, which is known to be the primary nonlinear mechanism for the breakdown to turbulence in the hypersonic boundary layer on solid surfaces, is completely absent on the porous surface. The fact that the ultrasonically absorptive coating suppresses this very dangerous nonlinear mechanism confirms the immense technological importance of this approach for hypersonic transition control where the second mode is dominant; this situation is encountered in the high-Mach-number flight of reentry vehicles.³

3) The degree of nonlinear phase locking that is associated with the subharmonic resonance, and identified on the solid surface, is substantially weakened on the porous surface. On the solid surface, the preferred subharmonic resonance increases in the downstream direction and therefore contributes to the early breakdown of the hypersonic boundary layer. However on the porous surface, there are no strongly preferred interactions associated with subharmonic modes; in fact these nonlinear interactions are observed to be weak

but persist farther downstream on the porous surface than on the solid surface.

4) The bispectral measurements presented here also identify a nonlinear interaction that is associated with the first mode; the previously made spectral measurements show the first mode is marginally destabilized by the ultrasonically absorptive coating. However this nonlinear interaction is observed to be very weak and has no deleterious effect on the performance of the ultrasonically absorptive coating.

The bispectral analysis improves our insight into the mechanisms of second-mode stabilization using an ultrasonically absorptive coating. It is thought that further substantial increases in the laminar run can be achieved by a suitable tailoring of the regular microstructure.

Acknowledgments

The first author gratefully acknowledges support from the European Office of Aerospace Research and Development, the Air Force Office of Scientific Research, and the U.S. Air Force Research Laboratory under Grant FA8655-03-1-5008. The work of three authors (D. Bountin, A. Shipliyuk, and A. Maslov) was supported by the European Office of Aerospace Research and Development under the International Science and Technology Center, Partner Grant 1863-2000.

References

- ¹Whitehead, A., "NASP Aerodynamics," AIAA Paper 89-5013, July 1989.
- ²Reshotko, E., "Transient Growth: A Factor in Bypass Transition," *Physics of Fluids*, Vol. 13, No. 5, 2001, pp. 1067–1075.
- ³Malik, M. R., "Hypersonic Flight Transition Data Analysis Using Parabolized Stability Equations with Chemistry Effects," *Journal of Spacecraft and Rockets*, Vol. 40, No. 3, 2003, pp. 332–344.
- ⁴Kimmel, R., "Aspects of Hypersonic Boundary Layer Transition Control," AIAA Paper 2003-0772, Jan. 2003.
- ⁵Fedorov, A. V., and Malmuth, N. D., "Stabilization of Hypersonic Boundary Layers by Porous Coatings," *AIAA Journal*, Vol. 39, No. 4, 2001, pp. 605–610.
- ⁶Rasheed, A., Hornung, H. G., Fedorov, A. V., and Malmuth, N. D., "Experiments on Passive Hypervelocity Boundary-Layer Control Using an Ultrasonically Absorptive Surface," *AIAA Journal*, Vol. 40, No. 3, 2002, pp. 481–489.
- ⁷Fedorov, A., Shipliyuk, A., Maslov, A., Burov, E., and Malmuth, N., "Stabilization of a Hypersonic Boundary Layer Using an Ultrasonically Absorptive Coating," *Journal of Fluid Mechanics*, Vol. 479, March 2003, pp. 99–124.
- ⁸Fedorov, A., Kozlov, V., Shipliyuk, A., Maslov, A., Sidorenko, A., Burov, E., and Malmuth, N. D., "Stability of Hypersonic Boundary Layer on Porous Wall with Regular Microstructure," AIAA Paper 2003-4147, July 2003.
- ⁹Kimmel, R. L., and Kendall, J. M., "Nonlinear Disturbances in a Hypersonic Boundary Layer," AIAA Paper 91-0320, Jan. 1991.
- ¹⁰Chokani, N., "Nonlinear Spectral Dynamics of Hypersonic Laminar Boundary Layer Flow," *Physics of Fluids*, Vol. 12, No. 12, 1999, pp. 3846–3851.
- ¹¹Shipliyuk, A. N., Bountin, D. A., Maslov, A. A., and Chokani, N., "Nonlinear Mechanisms of the Initial Stage of the Laminar-Turbulent Transition at Hypersonic Velocities," *Journal of Applied Mechanics and Technical Physics*, Vol. 44, Aug.–Sept. 2003, pp. 63–70.
- ¹²Shipliyuk, A. N., Bountin, D. A., Maslov, A. A., and Chokani, N., "Subharmonic Resonances in Hypersonic Laminar Boundary Layers," AIAA Paper 2003-0787, Jan. 2003.
- ¹³Kim, Y. C., and Powers, E. J., "Digital Bispectral Analysis of Self-Excited Fluctuation Spectra," *Physics of Fluids*, Vol. 21, No. 8, 1978, pp. 1452, 1453.
- ¹⁴Stetson, K. F., Thompson, E. R., Donaldson, J. C., and Siler, L. G., "Laminar Boundary Layer Stability Experiments on a Cone at Mach 8, Part 1: Sharp Cone," AIAA Paper 83-1761, July 1983.
- ¹⁵Lachowicz, J. T., Chokani, N., and Wilkinson, S. P., "Boundary-Layer Stability Measurements in a Hypersonic Quiet Tunnel," *AIAA Journal*, Vol. 34, No. 12, 1996, pp. 2496–2500.
- ¹⁶Kachanov, Y. S., and Levchenko, V. Y., "The Resonance Interaction of Disturbances at Laminar-Turbulent Transition," *Journal of Fluid Mechanics*, Vol. 138, Jan. 1984, pp. 209–247.
- ¹⁷Saric, W. S., Kozlov, V. V., and Levchenko, V. Y., "Forced and Unforced Subharmonic Resonance in Boundary Layer Transition," AIAA Paper 84-0007, Jan. 1984.
- ¹⁸Kosinov, A. D., Semionov, N. V., Shevelkov, S. G., and Zinin, O. I., "Experiments on the Nonlinear Instability of Supersonic Boundary Layers," *Nonlinear Instability of Nonparallel Flows*, edited by D. T. Valentine, S. P. Lin, and W. R. C. Phillips, Springer-Verlag, New York, 1994, pp. 196–205.

R. Lucht
Associate Editor